

# Influence of Sn substitution on amorphous to crystalline phase transformation in $\text{Ge}_{22}\text{Sb}_{22}\text{Te}_{56}$ chalcogenide films

J. KUMAR\*, R. THANGARAJ<sup>a</sup>, T. STEPHEN SATHIARAJ<sup>b</sup>

*Department of Physics, Arni University, Kangra, Himachal Pradesh, India*

*<sup>a</sup>Department of Physics, Guru Nanak Dev Univeristy, Amritsar-143005, India*

*<sup>b</sup>Department of Physics, University of Botswana, Botswana*

The effect of Sn substitution on phase transformation in  $\text{Ge}_{22}\text{Sb}_{22}\text{Te}_{56}$  (GST) chalcogenide system has been studied. Partial substitution of Sn upto 4 at% has been found to increase the phase transformation temperature of the GST. On further substitution of Sn (i.e. ~ 6 at %) the films were found to exhibit decreased phase transformation temperature. Optical study does not show any considerable change in optical band gap for Sn 2 and 4 at%. XRD investigation of annealed samples revealed that Sn substitution retains NaCl type crystalline structure of GST.

(Received October 17, 2011; accepted June 6, 2012)

*Keywords:* Ge-Sb-Te, Sn doping, Thin film, Chalcogenide phase transformation

## 1. Introduction

Present day data storage media stores the data in a single spot of amorphous phase in crystalline surrounding. Amorphous spot refers to digitally high value '1' whereas crystalline surrounding represents the digitally low value '0'. Depending on the mode of operation phase change storage media can be divided in to two categories (i) electrical erasable phase change memories (ii) optical phase change memories. In electrical erasable phase change memories an electrical current pulse is used to switch between amorphous and crystalline phases. It uses the difference in electrical resistance to store the data bit, because the phase change media shows very high resistance in amorphous phase than in crystalline phase. The optical data storage media takes the advantage of high difference between the reflectivity of amorphous and crystalline phase. A laser pulse is used to switch between the two phases. An amorphous spot in the crystalline surrounding act's as the stored bit.

Phase change materials, namely chalcogenides, play an important role in rewritable optical disks such as DVD-RAM and DVD±RW. The best chalcogenide materials in terms of storage density, speed and optical contrast were found to be  $\text{Ge}_{22}\text{Sb}_{22}\text{Te}_{56}$  (GST, used in DVD-RAM) and  $\text{AgInSbTe}$  (AIST, used in CD-RW and DVD + RW) [1, 2]. However, for high-definition (HD) television programs or video applications, we need to further increase both storage densities and data transfer rates. These requirements can be met with the help of dual-layer recording plus using a shorter wavelength laser. The doping of element Sn has been proposed by a group at Matsushita for this dual-layer recording at the blue-violet wavelength. The feasibility of rewritable dual-layer phase-change optical disk utilizing a blue-violet laser based on the Sn:GeSbTe material was demonstrated by T. Akiyama

et al. (2001)[3]. R. Kojima et al. (2001) demonstrated that Sn doped GeSbTe possesses a higher crystallization speed than GeSbTe, which is correlated to the single phase NaCl type structure of the GeSnSbTe material [4]. The influence of Sn doping should provide information how to improve the phase change behavior and development of new materials with better properties. In this work, we report phase change behavior of Sn doped  $\text{Ge}_{22}\text{Sb}_{22}\text{Te}_{56}$  chalcogenide material.

## 2. Experimental

Bulk  $\text{Sn}_x\text{Ge}_{22-x}\text{Sb}_{22}\text{Te}_{55}$  ( $x = 0, 2, 4, 6$ ) alloys were prepared by melt quenching technique. The constituent elements (99.999% purity) were weighed according to their atomic percentage and were sealed in a quartz ampoule (length ~10 cm, internal diameter ~6 mm), in a vacuum of  $\sim 10^{-5}$  mbar. The sealed ampoule was kept in a vertical furnace for 48 h and the temperature was raised to 1000 °C, at a rate of 4-5°C/min. The ampoule was rocked constantly to ensure homogeneous mixing of the melt. Ampoule was allowed to cool down at room temperature slowly. Ampoule was taken out of the furnace at room temperature and broken carefully to extract the sample.

Thin films of the above-mentioned compositions Sn:GeSbTe alloys were prepared by thermal evaporation method using Hind High Vacuum Coating Unit (Model No. 12A4D). Well cleaned glass slides were used as substrates. The substrates were maintained at room temperature during deposition and the pressure was below  $10^{-5}$  mbar in the chamber during the deposition. The films were left inside the vacuum chamber after deposition for 24 h to attain metastable equilibrium as suggested by Abkowitz (1984) [5]. The chemical compositions were

determined by using EDAX attached with Scanning Electron Microscope (Philips XL 30 ESEM system). The average composition of each thin film was obtained by measurement at three different regions of the film. The amorphous nature of the thin films was ascertained from the XRD spectra. The XRD spectra were obtained using Cu-K $\alpha$  radiation from PW3710 mpd controlled XRD system with a PW1830 generator. Absence of the sharp peaks in the XRD diffractograms confirms the amorphous nature of the bulk as well as thin films. The XRD study has also been performed on the films annealed above phase transformation temperature to reveal the structure of these glassy materials. The transmittance (T) w.r.t. air and specular reflectance (R) of thin films were measured at room temperature using UV-VIS-NIR spectrophotometer

(VARIAN Cary 500) in the 200-3000nm wavelength range.

### 3. Results and discussion

#### 3.1 Composition Analysis

The initial and actual compositions (obtained after EDAX analysis) for Sn $_x$ Ge $_{22-x}$ Sb $_{22}$ Te $_{56}$  ( $x = 2, 4, 6$ ) films are shown in Table 1. From the table, it is observed that the ratio of Ge/Sb in thin films is lower as compared to the initial composition taken for the preparation of bulk material. The Ge/Sb ratio also decreases with addition of Sn. This change in the relative composition leads to deficiency of Ge to form stoichiometric GST.

Table 1. Summarization of Initial composition, Actual Composition and Thickness for Sn $_x$ Ge $_{22-x}$ Sb $_{22}$ Te $_{56}$  ( $x=2, 4, 6$ ) thin films.

Samples With Initial compositions	Thickness of thin films ( $\mu\text{m}$ )	Samples With Actual compositions
Sn $_0$ Ge $_{22}$ Sb $_{22}$ Te $_{56}$	0.9913	Sn $_0$ Ge $_{14}$ Sb $_{35}$ Te $_{51}$
Sn $_2$ Ge $_{20}$ Sb $_{22}$ Te $_{56}$	0.6440	Sn $_2$ Ge $_{15}$ Sb $_{33}$ Te $_{50}$
Sn $_4$ Ge $_{18}$ Sb $_{22}$ Te $_{56}$	1.0900	Sn $_5$ Ge $_{11}$ Sb $_{38}$ Te $_{46}$
Sn $_6$ Ge $_{16}$ Sb $_{22}$ Te $_{56}$	0.9536	Sn $_6$ Ge $_{11}$ Sb $_{32}$ Te $_{51}$

#### 3.2 Temperature dependence of the sheet resistance

Temperature dependent sheet resistance measurements on the Sn:Ge $_{22}$ Sb $_{22}$ Te $_{56}$  film were performed to study the phase transformation temperature. The samples annealed up to 200°C under a vacuum better than 10 $^{-5}$  mbar. All these measurements were performed by recording the current values on regular temperature intervals. Fig. 1 shows the sheet resistance measurements of Sn $_x$ Ge $_{22-x}$ Sb $_{22}$ Te $_{56}$  ( $x = 0, 2, 4, 6$ ) films at a heating rate of 2.5 °C/min. The resistance decreases continuously in the lower temperature range until an abrupt drop appears at the temperature of ~125 °C. The reduction in sheet resistance upon the first transition is around three orders of magnitude. With further heating to 200 °C, the second drop is observed at a temperature of ~150 °C. The first phase analyzed were transformation temperatures obtained for Sn $_x$ Ge $_{22-x}$ Sb $_{22}$ Te $_{56}$  ( $x = 0, 2, 4, 6$ ) thin films were 104, 114, 120 and 104 °C also the second phase transformation temperatures obtained were 144, 162, 160 and 164 °C respectively.

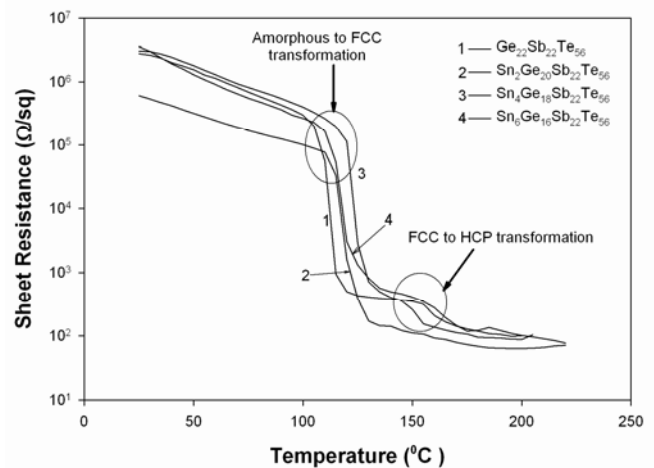


Fig. 1. Temperature dependent sheet resistance measurements of Sn $_x$ Ge $_{22-x}$ Sb $_{22}$ Te $_{56}$  (where  $x = 0, 2, 4, 6$ ) chalcogenide films.

### 3.3 X-ray diffraction studies

Fig. 2 shows the XRD scans for as-prepared and annealed  $\text{Sn}_x\text{Ge}_{22-x}\text{Sb}_{22}\text{Te}_{56}$  films for  $2\theta$  values ranging  $10^\circ$  to  $70^\circ$ . Curve (i) in each block belongs to the X-ray scan of as-deposited samples. Absence of sharp peak shows that the as-deposited films are in the amorphous state. Curve (ii) and (iii) belongs to the films annealed at 170 and  $225^\circ\text{C}$  for 10 minutes. The lattice parameter for composition  $\text{Sn}_2\text{Ge}_{20}\text{Sb}_{22}\text{Te}_{56}$  is determined to be  $6.022 \pm 0.004 \text{ \AA}$ , which is a little larger than  $6.014 \pm 0.016 \text{ \AA}$  for pure  $\text{Ge}_{22}\text{Sb}_{22}\text{Te}_{56}$ . Earlier studies reported the values of lattice parameter between  $5.988 \pm 0.008 \text{ \AA}$  and  $6.027 \pm$

$0.005 \text{ \AA}$  for pure  $\text{Ge}_{22}\text{Sb}_{22}\text{Te}_{56}$  [7]. For compositions  $\text{Sn}_4\text{Ge}_{18}\text{Sb}_{22}\text{Te}_{56}$  and  $\text{Sn}_6\text{Ge}_{16}\text{Sb}_{22}\text{Te}_{56}$  the values of lattice parameters determined are  $6.021 \pm 0.022$  and  $6.043 \pm 0.018 \text{ \AA}$  respectively. It is clearly evident that the lattice parameter increases with the increase in Sn concentration. It confirms that the first abrupt drop close to  $\sim 125^\circ\text{C}$  in the sheet resistance measurement corresponds to the transition to a NaCl-type structure (FCC) and the second abrupt drop close to  $\sim 150^\circ\text{C}$  corresponds to the transition to a HCP-type structure. Thus, it shows that the lattice parameters of the alloy will expand due to Sn doping, which is in agreement with the previous observation by Kojima and Yamada [4].

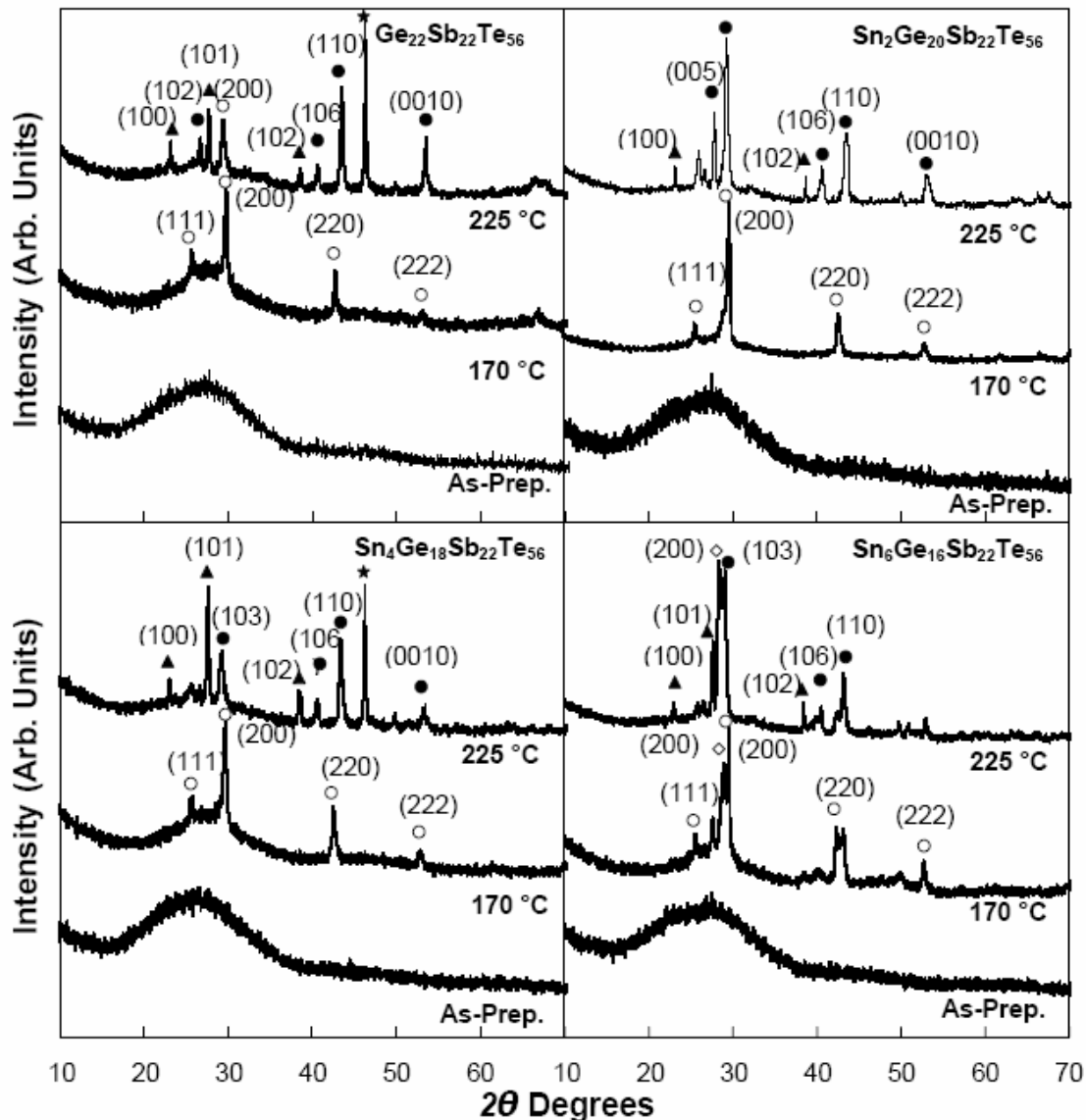


Fig. 2. X-ray diffraction scans of  $\text{Sn}_x\text{Ge}_{22-x}\text{Sb}_{22}\text{Te}_{56}$  ( $x = 0, 2, 4, 6$ ) films deposited on glass substrate performed on samples annealed at different temperatures. (◊) SnTe Phase, (★) Unknown peak, (▲) Te Phase, (●) GST hcp lattice, (◊) GST fcc Lattice.

Fig. 2 shows the absence of peaks corresponding to Sn rich phase for 2 and 4 at% of Sn, this indicates that

smaller amount of Sn, homogeneously mixes in the GST network and substitutes for the Ge position or vacancy,

leading to lattice expansion, which does not show there (Sn-phase) crystallization. Although absence of peaks (Sn-phase) can be caused by smaller sensitivity of X-ray method, not only by absence of new phase. However, for higher concentrations i.e, for 6 at% of Sn, sharp characteristic peaks of SnTe phase have been identified. This indicates the active participation of Sn in alloy formation. Thus, Sn might have compensated the disorder for lower concentrations. Since reduction in disorder always lead to more stable state, thus the resulting composition must be more stable, which is reflected in the higher value of phase transformation temperature in case 2 & 4 at% of Sn, as compare to pure GST. Although for 6 at% of Sn, the phase transformation temperature is somewhat lower side. The reason why the transition temperatures are lower can be explained in view of the different bond energies. The higher activation energy for crystallization is generally believed to be correlated with the stronger average bond energy. At this concentration Sn has been found to participate in bond formation. Replacing Ge by Sn should change this average bond energy and therefore, the crystallization temperature. The average bond energy is reduced by substituting the stronger Ge-Te (99.0 kcal/mol) bond for the weaker Sn-Te (86.0 kcal/mol) bond (Lide 1997). This may result in a lower phase transformation temperature as observed experimentally.

### 3.4 Optical properties

In order to determine the absorption coefficient ' $\alpha$ ' of the films reflection and transmission measurements were carried out at room temperature. In amorphous semiconductors, the optical absorption spectrum has been found to have three distinct regions viz., a high absorption region, the exponential edge region, and a weak absorption tail that originate from the defects and impurities. The higher absorption is caused by the band-to-band transition,

followed by an exponential Urbach tail and then finally, a weak absorption tail. It is well known that the weak absorption tail originates from the defects and impurities and the exponential region is strongly related to the characteristic structural randomness of amorphous materials, whereas, the high absorption region determines the optical band gap. In the strong absorption region, which involves optical transition between the valence and conduction bands, the absorption coefficient is given according to a model proposed by Tauc [8]. The absorption coefficient ( $\alpha$ ) of the films has been calculated from the transmission and reflection data using the relation

$$\alpha = \left( \frac{1}{t} \right) \ln \left\{ \frac{(1-R^2)}{(2T)} + \left\{ \frac{(1-R)^2}{(2T)^2} + R^2 \right\}^{1/2} \right\} \quad (1)$$

where ' $t$ ' is the thickness of the films, ' $T$ ' and ' $R$ ' represent transmission and reflection percentage respectively.

The spectral variations at room temperature for the absorption coefficient plotted as  $(ahv)^{1/2}$  vs. photon energy ( $hv$ ) for the as-deposited Sn:GeSbTe thin films are shown in Fig. 3. The linear relation of the  $(ahv)^{1/2}$  vs.  $(hv)$  plot indicates that the absorption mechanism in this system is a non direct transition [8]. The optical band gap for the nondirect transition can be obtained by the intercept of the above plots with the energy axis. The values of optical band gap obtained for Sn<sub>x</sub>Ge<sub>22-x</sub>Sb<sub>22</sub>Te<sub>56</sub> ( $x = 0, 2, 4, 6$ ) thin films were 0.59, 0.58, 0.59 and 0.48 eV respectively. Sn substitution does not show any considerable change in optical properties for Sn 2 and 4 at%. Although, for Sn 6 at% shows prominent drop in band gap value. The drop may be due to the formation of SnTe phase as is earlier identified by X-ray diffraction.

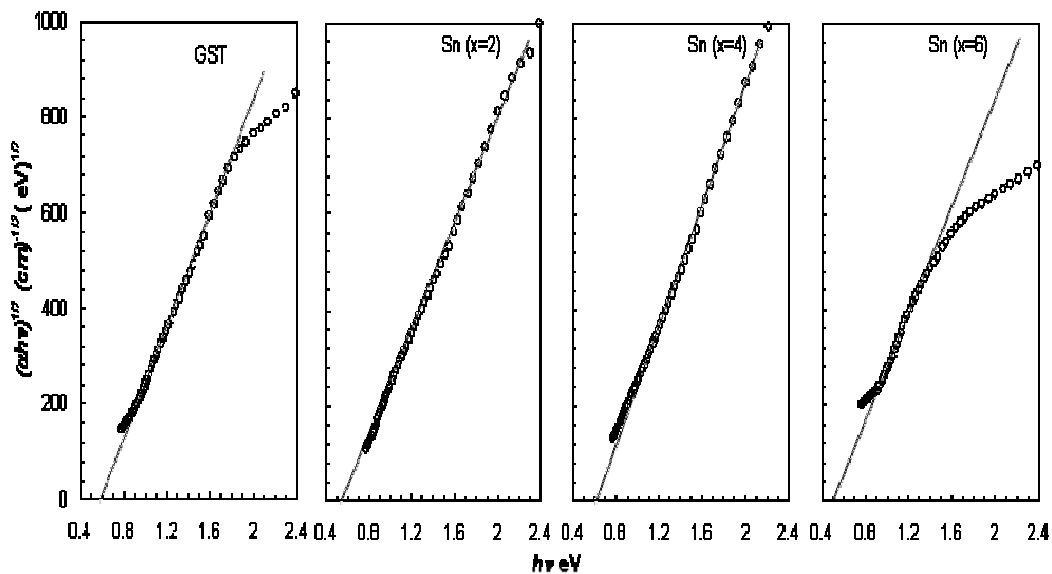


Fig. 3. Plots of  $(ahv)^{1/2}$  vs.  $hv$  for Sn<sub>x</sub>Ge<sub>22-x</sub>Sb<sub>22</sub>Te<sub>56</sub> ( $x = 0, 2, 4, 6$ ) thin films. The optical band gap  $E_0$  was obtained from the intercept on the energy axis of the plot.

#### 4. Conclusion

Thin films were prepared by thermal evaporation technique from the furnace cooled  $\text{Sn}_x\text{Ge}_{22-x}\text{Sb}_{22}\text{Te}_{56}$  ( $x= 0, 2, 4, 6$ ) alloy. Electrical, optical and structural investigations were carried out to understand the effect of Sn substitution in  $\text{Ge}_{22}\text{Sb}_{22}\text{Te}_{56}$  system. Electrical studies shows increase in phase transformation temperature with increased Sn substitution. Although, for Sn 6at% phase transformation temperature decreases slightly. This decrease has been correlated to the formation of weaker SnTe phase identified in Xray diffraction measurements. Formation of this phase is further found to decrease the optical gap for Sn 6 at%. It is concluded that lower Sn substitution not only retains the NaCl structure but also enhances the phase transformation properties of the material, whereas higher concentration of Sn (~6 at%) resulted in phase segregation and degrades the phase transformation properties.

#### References

- [1] J. H. Coombs, A. P. J. M. Jongenelis, W. van Es-Spiekman, B. A. J. Jacobs: *J. Appl. Phys.* **78**, 4906 (1996).
- [2] N. Yamada: *Mater. Res. Soc. Bull.* **21**, 48 (1996).
- [3] T. Akiyama, M. Uno, H. Kitaura, K. Narumi, R. Kojima, K. Nishiuchi, and N. Yamada: *Jpn. J. Appl. Phys.* **40**, 1598 (2001).
- [4] R. Kojima, N. Yamada: *Jpn. J. Appl. Phys.* **40**, 5930 (2001).
- [5] M. Abkowitz: *Polym. Eng. Sci.* **24**, 1149 (1984).
- [6] I. Friedrich, V. Wedenhof, W. Njoroge, P. Franz, M. Wuttig: *J. Appl. Phys.* **87**, 4130 (2000).
- [7] D. R Lide: *CRC Handbook of Chemistry and Physics* (Press, New York1997).
- [8] J. Tauc, *Amorphous and Liquid Semiconductors*. (London:Plenum Press1974).

---

\*Corresponding author: jitenderapd@gmail.com